Elucidating the role of the linker in DkTx mediated TRPV1 activation Mechanism

Submitted to

Indian Institute of Science Education and Research Pune

In partial fulfilment of the requirements for the

BS-MS Dual Degree Programme

By

Dheerendra Singh

Registration no. 20131138

Under Guidance of

Dr. Jeet Kalia

Indian Institute of Science Education and Research Pune
Dr. Homi Bhabha Road,
Pashan, Pune 411008, INDIA.

March, 2018

Certificate

This is to certify that this dissertation entitled "Elucidating the role of the linker in DkTx mediated TRPV1 activation mechanism" towards the partial fulfilment of the BS-MS dual degree programme at the Indian Institute of Science Education and Research, Pune represents work carried out by Dheerendra Singh at IISER Pune under the supervision of Dr. Jeet Kalia, Assistant Professor, Department of Chemistry during the academic year 2017-2018

Dheerendra
Signature of Student

Signature of Guide

COMMITTEE:

Name of guide: Dr. Jeet Kalia

Name of TAC: Dr. SaiKrishnan Kayarat

Dedicated to my parents

Who are with me in all difficult times

Declaration

I hereby declare that the matter embodied in the report entitled "Elucidating the role of the linker in DkTx mediated TRPV1 activation mechanism" are the results of the work carried out by me at the Department of Chemistry, Indian Institute of Science Education and Research, Pune, under the supervision of Dr. Jeet Kalia and the same has not been submitted elsewhere for any other degree.

Dhirendra

Signature of Student

Signature of Guide

Acknowledgments

I am feeling ecstatic while writing this thesis which is a prominent feat for me. This feat would not have been possible without the invaluable guidance provided to me by my guide Dr. Jeet Kalia, Assistant professor, IISER Bhopal, Department of Biology. He gave me sovereignty in the line of thought whenever I got in complications in experiments. He aided me when I could not solve an experimental complication that is why I am indebted to him for his invaluable contribution towards my thesis.

I particularly want to owe my thanks to Debayan Sarkar, a Ph.D. student with Dr. Jeet Kalia. He mentored me and assisted me in every minor experimental complication, and without him, it would be improbable for me to complete this thesis on time. I want to devote him my sincere gratitude for lending his helping hand in completing this thesis.

Last but not least, I sincerely admire the contribution of my lab mates Dr. Gregor Jose, Aditi Dixit, Yashaswi Singh, Rahul Nisal and Nitin Tagad and my colleagues from Dr. Sai Krishnan group and Dr. Gayathri group for extending their motivational approach, sympathetic attitude, special assistance and providing me essential chemicals required for my experiments.

ABSTRACT

Peptide toxins produced by venomous animals serve as powerful tools for unraveling the mechanisms of modulation of ion channel proteins they target. My thesis work focuses on studying the mechanism of activation of the transient receptor potential vanilloid 1 (TRPV1) ion channel by the double-knot toxin (DkTx), a toxin produced by the Chinese bird spider. Specifically, my work focuses on examining the as yet unexplored role of a seven residues-long “linker” region present in the toxin by generating variants of residues comprising this region of the toxin followed by their electrophysiological characterization as TRPV1 agonists. . Three types of toxin variants have been generated—site-directed substitutions of proline residues of the linker, truncations of the linker and substitution of all the residues of the linker to glycine residues. Functional characterization of these variants reveals that whereas proline substituents demonstrate negligible effects on toxin-activation of the channel, truncating the linker results in a profound alteration of both the wash-off rates and the potency of the toxin. Substituting all the linker residues with glycine results in a moderate effect on toxin activity. Taken together, these results demonstrate that the chemistry of the residues comprising the linker plays a minimal role in the toxin’s activity and that the linker primarily serves to provide the separation required for the two knots to reach out and concomitantly dock onto their binding sites on the channel.

CONTENTS

INTRODUCTION

Ion channels are membrane proteins that conduct ions through the membrane under the influence of environmental stimulus. Their roles in physiological mechanisms such as neuronal excitability and all cognitive functions make them indispensable components of the cellular proteome. Due to their involvement in numerous physiological processes, these are also important drug targets. Among several other ligands that serve as agonists or antagonists of ion channels and receptors, animal toxins are of paramount importance whether they are small molecule toxins or complex peptide toxins. Not only toxins have contributed tremendously to structure-function studies on channels and receptors, but they have also served as attractive leads for drug design. Indeed, research on toxin modulation of channel function has attracted a significant amount of interest over the last four decades in areas as diverse as proteomics, structural biology, and pharmacology. My thesis work focuses on the double-knot spider toxin (DkTx)—a recently discovered selective agonist of the transient receptor potential vanilloid type 1 (TRPV1) ion channel.

The physiological role of TRPV1 and its subtypes

Ion channels constitute a large percentage of the membrane-bound proteome of the cell. Membrane proteins categorically constitute three types of proteins: integral membrane proteins, peripheral membrane proteins, and lipid-anchored membrane proteins. The large family of ion channels is categorized under the integral membrane proteins. Transient Receptor Potential (TRP) channels, a large class of ion channels, are non-selective cation channels. There are seven types of TRP channels, namely - TRPML (mucolipin), TRPM (melastatin), TRPA (ankyrin), TRPP (polycystin), TRPN (no mechanoreceptor potential C (NOMPC)- like) and TRPV(vanilloid) channels. Mutations in these channels have reportedly resulted in several neurodegenerative disorders and other non-neurogenic diseases in humans (Nilius and Owsianik, 2011). Transient Receptor Potential Vanilloid (TRPV) are subtypes of TRP channels; this TRPV are further classified into six subtypes, TRPV1-6 (Nilius et al., 2007).Mutation in every TRPV subtype have been associated with neurodegenerative disorders. (Nilius et al., 2007)(For example, gain-of-function mutations G573S and G573C in the S4-S5 linker and W692G in TRP domain of TRPV3 can cause a rare congenital disease called Olmsted Syndrome(Lin et al.,

2012). A gain-of-function mutation in the TRPV4 S4-S5 linker can cause skeletal dysplasia syndrome (Loukin et al., 2011). Out of all TRPV subtypes, TRPV1 has been best-studied to date and has been thoroughly characterized as heat and capsaicin-activated channel (Caterina et al., 1997).Mutations in this channel can lead to various diseases, for instance, mutations in mice TRPV1 that render it hypofunctional can cause diseases such as diabetes and obesity(Suri and Szallasi, 2008). Furthermore, other mutations in TRPV1 can cause diseases like renal hypertension, allodynia, irritable bowel diseases, asthma, bladder disease and migraine (Nilius et al., 2007).TRPV1 is also an attractive drug target as demonstrated by the use of PAC-14028, a TRPV1 antagonist currently undergoing phase 1 clinical trial on humans after completed good laboratory practices (GLP) preclinical packages for treating pruritus and atopic dermatitis (Lim and Park, 2012).

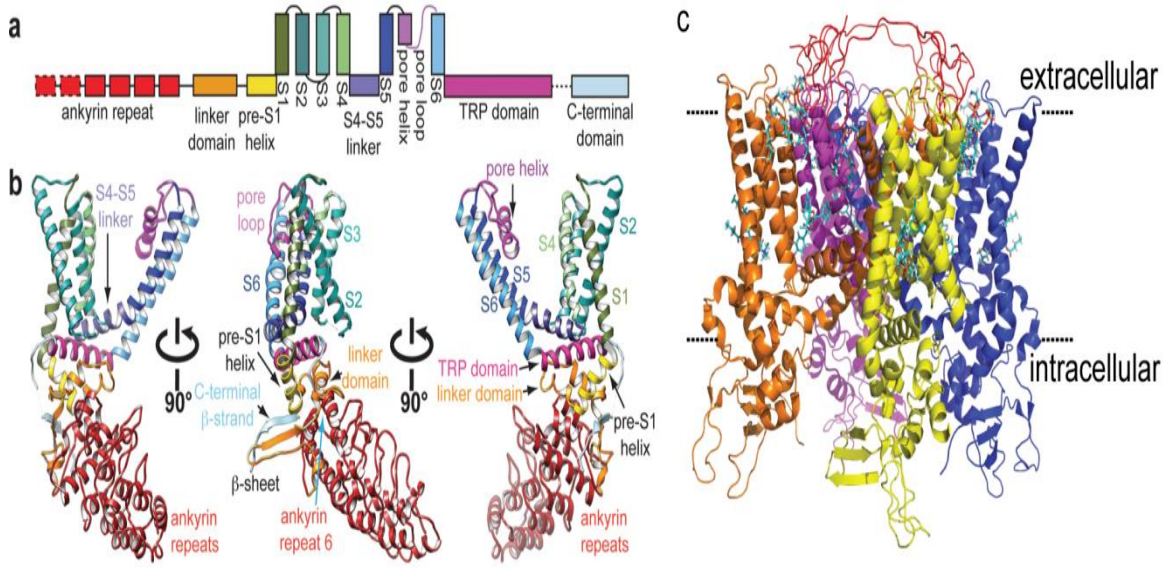

Figure 1: **Side-view of single subunit structure and complete tetrameric of TRPV1. a**. Schematic representation of the domains in the rat TRPV1 channel.(Adapted from Liao et al., 2013) **b**. Single subunit structure viewed three angles perpendicular to each other.(Adapted from Liao et al., 2013) **c.** Side-view of homotetrameric TRPV1 channel bound to DkTx.

Toxins as Pharmacological tools to decipher structure and function of membrane-bound channels

Ludwig Brieger, an organic chemist in the 19th century, coined the term toxins when he discovered the generation of toxic material from the growth of typhoid *Bacillus* known as typhotoxin (Brieger L, et al., 1890 and Brieger L, et al. 1883). Ion channels and ligand-gated voltage channels are very important for most of the living being for

transport of vital ions through the cell membrane, and simultaneously these channels can be used to fire neurotransmitters that carry important signaling in the nervous system (Hille,2001). Since ion channels have such important physiological roles, macromolecules of biological or non-biological origin can be used to target these membrane channels for pharmacological purposes to get vital insights of these membrane channels. Toxins have been historically proven to be very useful in deciphering structure and function of membrane channels(Adams and Olivera, 1994).Most toxins from different venomous plants and animals known to modulate ion channels either in open state or closed state to defend themselves from a predator or to catch the prey (Mebs, 2002). Some of the toxins which have been isolated from fishes, snails, spiders, snakes, and octopus has been shown to modulate membrane-bound channels and receptors, they have hence been used to perform structural and functional studies on several of these channels and receptors, such as, $K_v$channels, Na_v channels, Acid-sensing ion channels and Nicotinic acetylcholine receptors (Kalia et al., 2015). Toxins are usually categorized, based on site of binding, as two different types – one that binds to the peripheral regions of the channel and modulates the gating movements in the same; another type binds directly to the pore region of the channel and interacts closely with the ion permeation pathway. The former type of toxins are known as the gating-modifier toxins, and the latter type is known as the pore-binding toxins (Bae et al., 2016; Milescu et al., 2007).Among the gating modifier toxins, paddle toxins are the have been most extensively studied. Many paddle toxins have been isolated from the venoms of spiders, scorpions, and other venomous animals. These toxins have been named so because they bind to a structural motif present in the voltage sensor of voltage-gated ion channels known as the paddle motif and prevent the voltage sensor from undergoing the conformational change required for the opening of the channel pore. The other group of toxins, which are the pore-binders bind close to or inside the ion permeation pathway and occlude the passage of ions physically. Examples of such pore-blocking toxins include charybdotoxin that acts on K_v channels (Goldstein et al., 1994) or μ-conotoxins that act on Ca_v channels (McGivern, 2007).There are several toxins which offer therapeutic potential and one of these μ-conotoxins that block Ca_v channel is now in the market as a drug named Ziconotide. Ziconotide is a peptide toxin isolated from the fish-eating snail. It functions as a painkiller in acute pain and can be a substitute for morphine as it

blocks N-type voltage-gated calcium channels at the pore regions occluding the ion permeation pathway. (McGivern, 2007).The recently discovered double-knot toxin (DkTx), a TRPV1 channel agonist, is the only known pore-binding toxin that functions as a channel activator(Bohlen et al., 2010). This toxin has contributed tremendously to TRPV1 biology by facilitating the solving of the cryo-EM structure of the channel in the complex (Gao et al., 2016 and Cao et al., 2013).

Structure of TRPV1 and DkTx and their binding mechanism

Toxins can be employed to trap channels in specific conformational states. Utilizing this property, toxins have been employed to obtaining snapshots of channel structures in different states of gating. A similar strategy was employed to obtain the TRPV1 structure by using various toxins and small molecules such as Resiniferatoxin (RTX), Double knot toxin (DkTx), small vanilloid molecules like capsaicin, lipids like PIP_2. (Cao et al., 2013)TRPV1was first cloned by David Julius's group in 1997 to be discovered primarily as a capsaicin-sensing channel. Structurally it was predicted to be composed of six transmembrane helices, and the pore region was predicted to be between the fifth and sixth transmembrane helices, employing hydrophilicity analysis based on the Hopp-Woods algorithm (Caterina et al., 1997).The first cryo-EM structure of TRPV1 was elucidated in 2008 at a resolution of 19 Å, which revealed the channel's four-fold symmetry and the topology of C-terminal and N-terminal cytoplasmic region (Moiseenkova-Bell et al., 2008). Recently, structures of TRPV1 have been solved to a resolution of up to 2.9 Åusing single-particle cryo-electron microscopy and also by using scaffolding proteins in lipid nanodiscs which mimic native membrane-like environment. (Cao et al., 2013; Liao et al., 2013). TRPV1 is a homotetramer channel which consists of N-terminal ankyrin repeats that are localized towards the cytosolic side of the membrane. Ankyrin repeats are present in many TRP channels, especially being the signature domains for TRP Ankyrin type of channels, eg., TRPA1 channels(Gaudet, 2008).There are six ankyrin repeats in each of the TRPV1 monomers which form assembly domain within the cytoplasmic N- terminal domain. ARDs have also been attributed to the function of ATP binding and Ca^{2+} mediated desensitization mechanism.(Inada et al., 2012; Liao et al., 2013a). TRPV1 channel shares homology regarding structural topology with voltage-gated potassium channels even though

TRPV1 channel exhibits very little (<20%) sequence homology to Voltage-Gated Ion Channels (VGICs). Apart from TRPV1's six transmembrane helical domains (S1-S6) that span over lipid bilayer similar to VGICs, TRPV1 has pore helix and pore re-entrant loop found between S5-S6 helix which too shares similar configuration that is seen in VGICs (Figure 1a, b)(Liao et al., 2013). In VGICs S1-S4 domain act as the voltage sensing domain, specifically S3 and S4 helices that contain charged residues.Even though resembling the topological homology, TRPV1 S1-S4 domains are relatively stationary to VGICs and contain hydrophobic residues, which if were to be mutated, can lead to the non-functional channel (Boukalova et al., 2013; Payandeh et al., 2011). TRPV1 also contains a TRP domain which is located just after the S6 helix and which contains about 23-25 amino acids. This domain can be found in many TRP channels and can be considered as a signature domain for TRP channels (Ramsey et al., 2006). Outer pore region of TRPV1 is wide open as compared to voltage-gated sodium channel (Na_v) and it is located between S5 and S6 helix it contains selectivity filter, pore helix, and pore loop (Figure 1a, b). Selectivity filter is narrow has a diameter of around 6 Å (Susankova et al., 2007). Even though selectivity filter is narrow, it dilates when the channel gets activated, and it can even allow large cations to permeate when the channel is subjected for prolonged activation (Chung et al., 2008). Down the pore region of the channel, residue I679 emanating from S6 helices of all four homotetramers come together to form a very constricted hydrophobic seal which has a diameter of 5.3 Å around the central ion pathway formed by a pore loop, S5, and S6 transmembrane helices (Liao et al., 2013). In summary, as depicted in Fig. 1,each subunit of TRPV1 contains 6 ARDs, a linker domain, a pre-S1 helix, S1-S4 transmembrane domains, S4-S5 linker, S5-S6 transmembrane domains and in between this domain a pore helix and a pore loop and characteristic domain of TRP channels, a TRP helix(Figure 1a, b, and c).

Double Knot toxin (DkTx), a member of the family of ICK (Inhibitory cysteine knots) toxins, was discovered in the venom of Chinese eating bird spider *O. huwena*(Bohlen et al., 2010). DkTx posses two ICK knots (named K1 and K2 knots) connected by a seven amino acids-long linker region, consisting of a total of 75

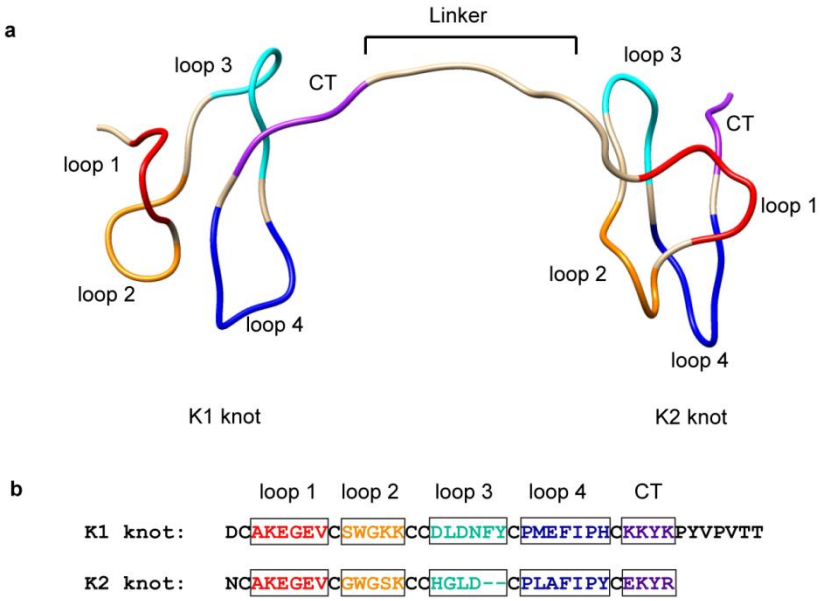

Figure 2: **DkTx structure and sequence alignment of the two knots. a.** DkTx structure from the cryo-EM structure (PDB id: 5irx). All loops and carboxyl-terminal designated in specific colors – showing loop1 in red, loop 2 in golden, loop 3 in cyan, and loop 4 in blue and CT (C-terminus) in purple.**b.** Sequence alignments of the K1 and the K2 knots with the loops and C-terminus colored with the same color scheme.

amino acids. DkTx activates the TRPV1 channel with very slow dissociation kinetics (Bae et al., 2012;Bohlen et al., 2010). Distributions of cysteine residues in the DkTx peptide sequence shows high similarity to other ICK toxins which determines the resultant folding pattern of the toxin (Figure 3b)(Bae et al., 2012; Bohlen et al., 2010).Recombinant DkTx folds efficiently *in vitro* in the presence of non-ionic detergents and its retention time in the folded form increases compared to the linear peptide in reverse-phase liquid chromatography indicating that DkTx is more hydrophobic in its folded form (Bae et al., 2012). Furthermore, it is also known that the two knots can fold independently and are TRPV1 agonists, though with a poorer potency and faster dissociation properties (Bae et al., 2012; Bohlen et al., 2010). The NMR structure solved of the DkTx shows three disulfide bonds in each of the DkTx knots which stabilize their tertiary structure (Figure 3a). (Bae et al., 2016) Both knots have antiparallel β-sheets stabilized by disulfide bonds in each of the two knots. Like many other ICK toxins, both K1 and K2 demonstrate exposed hydrophobic interfaces that are surrounded by acidic and basic residues which are indicative of its amphipathic nature. Both the knots of DkTx share high sequence homology barring loop 3 (as shown in Figure 2), which in the case of K1 is longer than that of K2 (Bae et al., 2016). Molecular dynamics simulations and docking studies performed by Dr.

Kenton Swartz's group suggests that the tryptophan residue in loop 2 of K1 (figure 2) is more solvent accessible than the equivalent residue of the K2 knot (Bae et al., 2016). These tryptophans seem to play a crucial role in the toxin-channel interactions that are mediated by lipids (Bae et al., 2016; Gao et al., 2016; Sarkar et al., unpublished data).In summary, DkTx consists of two knots K1 and K2 both being hydrophobic and amphipathic like other ICK toxins (Figure 2) (eg., SGTx1, GxTx1E) which modulate voltage-gated potassium channels.(Garcia et al., 2000; Lee et al., 2004) Each knot consists of three disulfide bonds, four loops, and two short antiparallel β-sheets which remain to be only defined secondary structures present in the toxin structure (Figure 3a,2)(Bae et al., 2016; Gao et al., 2016)

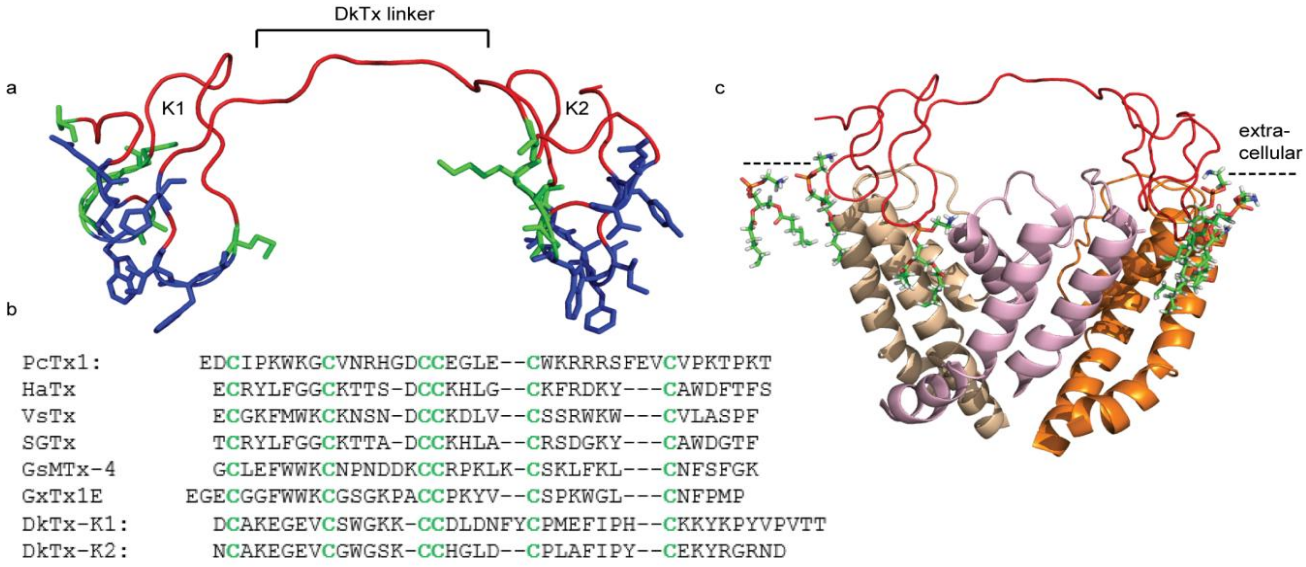

Figure 3: **DkTx structure and DkTx-lipid-TRPV1 tripartite complex**. **a.** DkTx cryo-EM structure shown in cartoon format. Backbone is shown in red, lipid-interacting residues in blue and exclusively channel interacting residues in the green of K1 and K2 knots. Seven amino acid long DkTx linker demarcated on top. **b.** Peptide sequence alignment of DkTx K1 and K2 knots with other inhibitor cysteine knot toxins. Conserved cysteines marked in green color. **c.** DkTx-lipid-TRPV1 tripartite complex shown in the zoomed-in view. Different channel monomers are colored in separate colors. DkTx is colored red, and lipids are shown in stick representation.

DkTx binds to the outer pore domain of TRPV1 in a counter-clockwise direction located between S5 and S6 transmembrane helices (Figure 3c).Our research group has been working on the TRPV1 activation mechanism by DkTx, where we have learned that the lipid-interacting residues of the DkTx that either interact with the channel pore or not play a crucial role in stabilizing the interaction between the

channel and the toxin, resulting in such phenomenally slow wash-off kinetics. It was surprising to observe that the lipid-interacting residues of K1 knot play a much significant role compared to their K2 counterparts in the binding affinity of the toxin. We have also learned that the K1 variants that dissociate faster also show poor lipid-partitioning, compared to their K2 counterparts (Sarkar et al., unpublished data). My research project has focussed on another structural moiety of DkTx, the seven amino acids-long linker that connects the two knots of the toxin. I have explored the role of the linker length, chemistry, and rigidity in the binding mechanism, as well as the proposed bivalency mode of binding. To achieve this goal, I have generated variants of linker residues and have also modulated the linker length by deleting residues of the linker. I have then characterized the activity of the resulting toxin variants by performing two-electrode voltage clamp recordings.

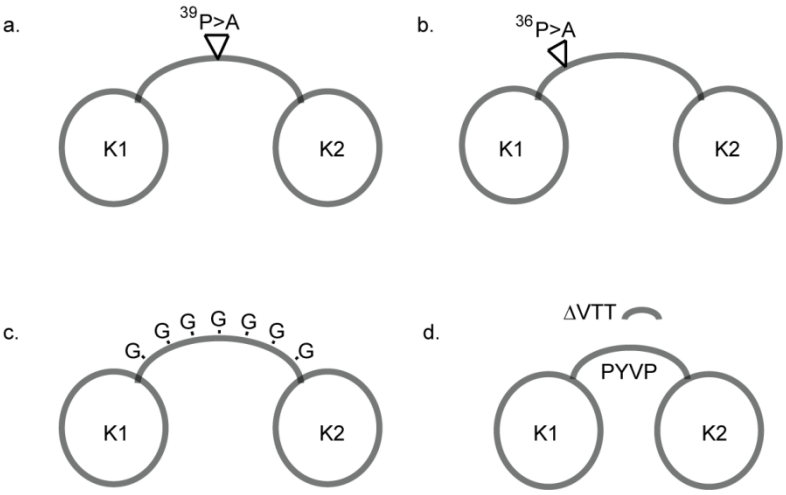

Figure 4: Research design for investigating role of linker in DkTx - mediated TRPV1 activation mechanism. **a.** Alanine substitution at 39th Proline, **b.** Alanine substitution at 36th Proline, **c.** Replacement of PYVPVTT with 7 Glycines and **d.** deletion of three amino acids (VTT) from linker.

Materials and Methods

1. PCR

We performed whole-plasmid site-directed mutagenesis and Restriction-free (RF) cloning to amplify DkTx gene. For whole-plasmid site-directed mutagenesis, I have used a forward primer (F.P.) and reverse primer (R.P.) complementary to a template construct (pET31b vector containing DkTx gene downstream of keto-steroid isomerase [KSI]). These primers would bind to their complementary sites with the site of mutation looping out, but yet extend to the whole plasmid, i.e., a pET31b vector containing KSI-DkTx fusion gene. In RF method, we designed a pair of primers similar to the whole-plasmid site-directed mutagenesis, and another pair

primers that complement sequence of DNA stretches flanking the KSI-DkTx fusion gene.The resulting PCR products would be megaprimers which were then used to amplify the entire plasmid containing KSI-DkTx fusion gene to obtained desired full-length amplicon which was then used for *DpnI* digestion followed by transformation into *E.coli* NEB Turbo cells (Figure 5). Primer sequences for the constructs made are given in *Appendix 1*. PCR amplification reactions were performed using Phusion DNA polymerase (Thermoscientific Inc.) using PCR cycles mentioned in *Appendix 2*. Clone for the 7G DkTx was provided generously by Dr. Kenton Swartz (NINDS, NIH, USA).

2. Cloning

Following PCR reactions to incorporate mentioned substitutions in the DkTx gene, the PCR products were treated with *DpnI* overnight at 37˚C to cleave any methylated parental plasmid present in the PCR mix. *DpnI* digested PCR mix of all the above three mutants were transformed into *E.coli* NEB Turbo chemically competent cells and selected for transformants on LB-ampicillin plates. Transformants obtained were then inoculated with 6 ml of culture containing ampicillin (100 µg/ml) and then incubated at 37˚C for 12 hours. Plasmid purification was performed using Qiagen plasmid isolation kit and sent for sequencing to 1st Base Asia. Representative gel images of whole-plasmid site-directed mutagenesis and RF cloning has been shown in Figure 5.

3. Protein production

After obtaining a confirmed clone of the mutants mentioned above, resultant mutant plasmids were transformed into *E.coli*BL21 (DE3) cells and incubated at 37˚C overnight to obtain transformants on LB-ampicillin plates. These isolated colonies were used to inoculate six mL LB-ampicillin broth to obtain a primary culture of the transformed*. E. coli* BL21 (DE3) cells. The primary culture (2 mL) was used to inoculate in large cultures of 1 liter, and induction was performed at a final concentration of 0.5 mM IPTG at $O.D._{600}$of ~0.4-0.6, as DkTx gene was under the control of lac promoter. The cells were then incubated at 37˚C for 6-8 hr before harvesting these cells by centrifuging at 5,500 RPM for 20 minutes. This pellet was

then resuspended in 20 mM Tris-HCl(pH 8.0) and then were ultrasonicated. The resultant cell lysate was centrifuged at 12,000 RPM for one hr. The supernatant was discarded, and the cell pellet was dissolved in 6 M Guanidine HClsolutionovernight. Hydroxylamine was added at a final concentration of 2 M to this solution, and the pH of the solution was adjusted to 9 with 10 N NaOH and incubated at 45 ˚C for 4.5 hours to facilitate peptide bond cleavage between “Asn-Gly,” present at the interface of the KSI-DkTx fusion protein. Dithiothreitol (DTT) was added to a final concentration of 300 mM, and then the solution was incubated for one hr at 45 ˚C to break all possible disulfide bonds of the misfolded peptide. The reaction was stopped by adjusting pH to 4 by adding concentrated HCl. This entire solution was then centrifuged for 30 minutes at 18,000 RPM, and the supernatant was then dialyzed for against water (containing 0.1%TFA). This dialysate was then frozen in liquid nitrogen and then lyophilized to obtain white powdery linear peptide.

4. Protein refolding and Purification

After lyophilization, the linear peptide was dissolved in acetonitrile containing 0.1% Trifluoroacetic acid (TFA) to a final concentration of 2 mg/ml and stored in 4˚C. This dissolved linear DkTx peptide then added to refrigerated refolding buffer (pH 8.0) consisting of 0.4 M Tris-HCl, 1mM EDTA, 0.5% Triton X 100, 2.5 mM reduced glutathione (GSH) and 0.5mM oxidized glutathione (GSSG) to refold *in vitro* at 4˚C for 2 days to obtain refolding peptide. The refolding of DkTx protein progression was monitored by using Agilent 300SB-C18 column under Reverse-Phase (RP) HPLC conditions using a linear gradient of 5-65% acetonitrile (containing 0.1%TFA) over a period of 30 minutes. Refolding traces of toxin variants has been demonstrated in Figure Q. On obtaining sharp peak of the fully oxidized peptide on HPLC and analyzed mass by Matrix Assisted Laser Desorption-Time Of Flight (MALDI-TOF) mass spectrometry, the refolding reactions were quenched adjusting pH to 4 by titrating against concentrated HCl. The refolding solution was then reverse-dialyzed against 400 g/L of PEG20 solution to concentrate the solution for HPLC purification using the same linear solvent gradient as above. Pure refolded protein (depicted in Figure 9) was then quantitatively analyzed by UV spectrometry at 280 nm and then aliquoted as 1nmolfraction and vacuum-dried to be used for electrophysiological assays or to be stored at -80˚C.

5. *Xenopus laevis* surgery and extraction of oocytes

Female *Xenopus laevis* was anesthetized to remove stage 5 or 6 oocytes are surgically abiding by the protocol for surgery approved by Institutional Animal Ethics Committee (IAEC), IISER- Pune.

6. Oocytes preparation and Two-Electrode Voltage Clamp (TEVC) electrophysiology

Surgically removed oocytes were defolliculated after treating them with collagenase type II enzyme to a concentration of 2mg/ml in Calcium OR2 buffer containing 1mM $MgCl_2$, 82.5mM NaCl, 2.5mM KCL, and 5mM HEPES at pH 7.6. Oocytes were then injected with cRNA of rat TRPV1 with a volume of 50nl per oocyte. This rat TRPV1 cRNA was produced by *in vitro* transcription from *NotI* cleaved linearized rat TRPV1 DNA cloned in pGEM HE vector by using HiScribe T7 ARCA mRNA kit (New England Biolabs Inc.). Injected oocytes were then transferred to the ND96 solution (pH 7.6) comprising 96 mMNaCl, 1vmM $MgCl_2$, 5 mM HEPES, 50 µg/ml Gentamycin, 2mMKCl, and 1.8 mM $CaCl_2$have been kept at 18˚C for 1-2 days to let the expression of TRPV1 protein channel in oocytes. Recording buffer solution (pH 7.4) comprising of 50 mMKCl, 50 mMNaCl, 0.3 mM $BaCl_2$, 1 mM $MgCl_2$ and 20 mM HEPES was used to record the current from TRPV1 channel evoked by the toxin. TEVC recordings on TRPV1 expressing oocytes were performed in a 150 µl recording chamber. By using digi data analog to digital converter and pClamp software (Molecular Devices), the recorded data was filtered and digitized at 0.5 kHz and 2.5 KHz respectively. Two microelectrodes, filled with 3 M KCl of resistance between 0.1 to 1 MΩ, were used as voltage and current electrodes. While recording, oocyte kept in recording buffer was impaled with both electrodes and clamped at -60 mV. After checking the initial leak current, first capsaicin was perfused onto the oocyte at a final concentration of 5 µM (prepared in recording buffer). After capsaicin saturation current had reached, recording buffer is perfused in the chamber to wash-off the capsaicin, and on reaching basal current, the wild-typeDkTx or its variants were pipetted into the recording chamber. The toxin current evoked by variants and capsaicin were recorded and analyzed using Clampfit 10.5 software (Molecular Devices) (Figure9). Oocytes were subjected to a different concentration of toxin variant and recorded at each concentration for minimum 3 times.

7. Electrophysiological Data Analysis

To generate dose-response curve the normalized ratio of toxin evoked current and the capsaicin-evoked current was plotted against different toxin concentration. The plot was fitted to a Hill equation given below in Origin 9.0.

$$y = A_{max}\ \{(x^n)/(j^n + x^n)\}$$

Where, A_{max} is the normalized maximal ratio of toxin evoked current and capsaicin (5 μM) evoked current, 'n' is the hill coefficient and 'j' is EC50. The dose response curves of the toxins have been shown as Figure 9 in the Results section.

8. Wash-off kinetics data analysis

Percentage of the ratio of the difference in magnitude of current after 3 minutes of toxin wash-off to the magnitude of maximal current induced by toxin at saturation concentration of the wild-type or other toxin variants was taken as the measure of toxin wash-off kinetics. The toxin current traces were analyzed to extract magnitude of current using the Campfit 10.5 software (Molecular Devices) for percentage wash-off calculation. Toxin wash-off kinetics has been shown as "% wash-off in 3 mins vs. toxin (saturation concentration)" in Figure 10 in the Results section.

Results

The structural and functional studies (Gao et al., 2016; Bae et al., 2016; Cao et al., 2013; Bae et al., 2012; Bohlen et al., 2010) on DkTx published thus far have not provided any detailed insights into the into the role of the linker region in the DkTx toxin.To understand the role of the linker in DkTx-mediated TRPV1 activation mechanism we asked, what is the role of the two prolines in the linker peptide sequence? Does it confer rigidity of any sort? Does the exact sequence of the linker have any specific role to play or any random hepta-peptide can replace it? Is the linker length evolutionarily chosen to be seven amino acids or can larger or shorter linker can also perform the desired function?

To answer whether the prolines are important for linker rigidity and thus for DkTx function, I mutated the P36 and P39 to alanine as single amino acid substitution variants. To delineate whether seven amino acids is the optimal length for the double knot toxin to function normally, I constructed the ΔVTTmutant, which is a three

amino acid deletion variant of the linker of DkTx (Figure 4). The 7G DkTx, obtained from Swartz lab was examined to address the importance of chemistry and the structure of linker residues.

Cloning of DkTx variants:

I cloned the P39A and P36A variants of DkTx in the pET31b construct containing KSI-DkTx fusion protein by employing whole-plasmid site-directed mutagenesis method. To achieve the same, I used each of the mutants forward and reverse primers together with the KSI-DkTx construct the template. The PCR reactions

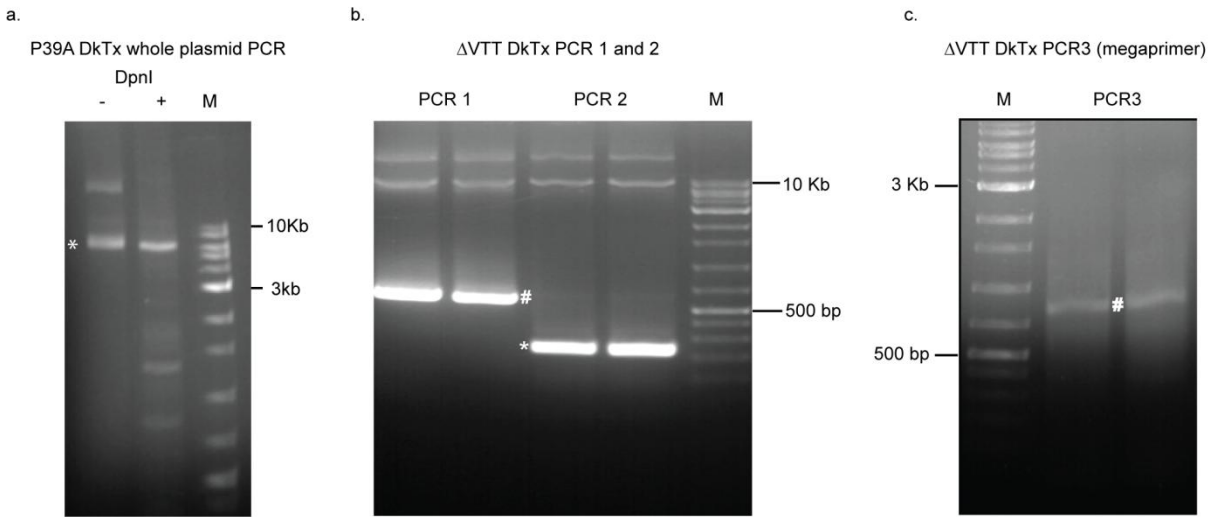

Figure 5: PCR reaction gels for whole-plasmid mutagenesis and restriction-free cloning. **a.** P39A DkTx PCR amplicon (~6 kb marked as*) shown before and after DpnI digestion shown on 1% agarose gel. **b.** ΔVTT DkTxPCR 1 and 2 reactions run on 1% agarose gel. # demarks 629bp band of PCR 1 and * demarks 245 bp of PCR2. **c.** PCR 3 product ofΔVTT DkTx (804 bp band denoted as #)

primers together with the KSI-DkTx construct the template. The PCR reactions were optimized for the annealing temperature based on the primer melting temperatures (60˚C for P39A primer pair and 52˚C for P36A primer pair) (Figure 5a). For the ΔVTT construct whole-plasmid site-directed mutagenesis PCR did not work. Hence RF cloning was employed for the same. There were total four reactions involved in this method: PCR1 performed with the template plasmid, mutant reverse primer and 5'-flanking forward primer NdeIF and PCR2 with the 3'-flanking reverse primer, BlpIR and the mutant forward primer (refer *Appendix 1* for primer sequence). Amplicon from both PCR1 and PCR2 in equimolar proportion was used for the PCR3 reaction, which resulted in the ΔVTTmegaprimer (Figure 5b, c). This megaprimer was

subsequently used to amplify the whole plasmid template to generate the mutant amplicon. All the above whole-plasmid PCR amplicons were subjected to *DpnI* digestions at 37˚C overnight and were transformed into *E.coli* NEB Turbo cells and grown on LB-ampicillin plates as mentioned in '*materials and methods*' section. Isolated plasmids from these transformants were sent for sequence confirmation and the plasmids containing correct mutant sequences were transformed into *E.coli* BL21(DE3) cells for protein expression.

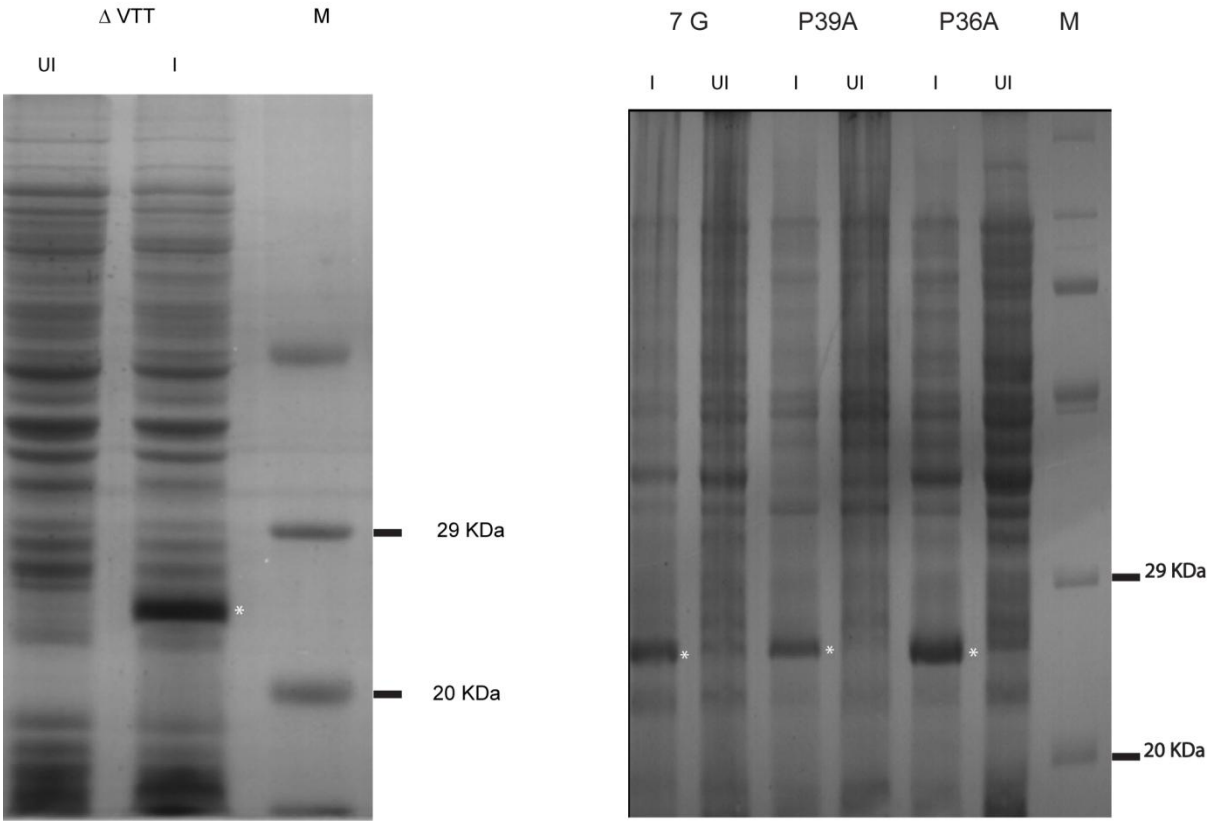

Figure 6: IPTG induction of KSI-DkTx linker variants fusion proteins. IPTG induced over-expressed protein band (~24 kDa) is depicted with an asterisk in the induced 'I' lane. 'UI' and' denotes uninduced and molecular weight marker lanes respectively.

Production of wild-type DkTx and its variants:

KSI-DkTx fusion gene, which was engineered to be present downstream to the *lac* promoter was induced by IPTG (0.5 mM) in 1 L cultures at an $O.D._{600}$ or 0.4-0.6. Following 6-8 hours of incubation with IPTG, the culture was centrifuged at 5500 rpm for 20 minutes to collect the culture pellet. To check for protein over-expression, equal cell density of bacterial culture before and after IPTG induction was subjected to SDS-PAGE analysis, where I demonstrated over-expression of the desired

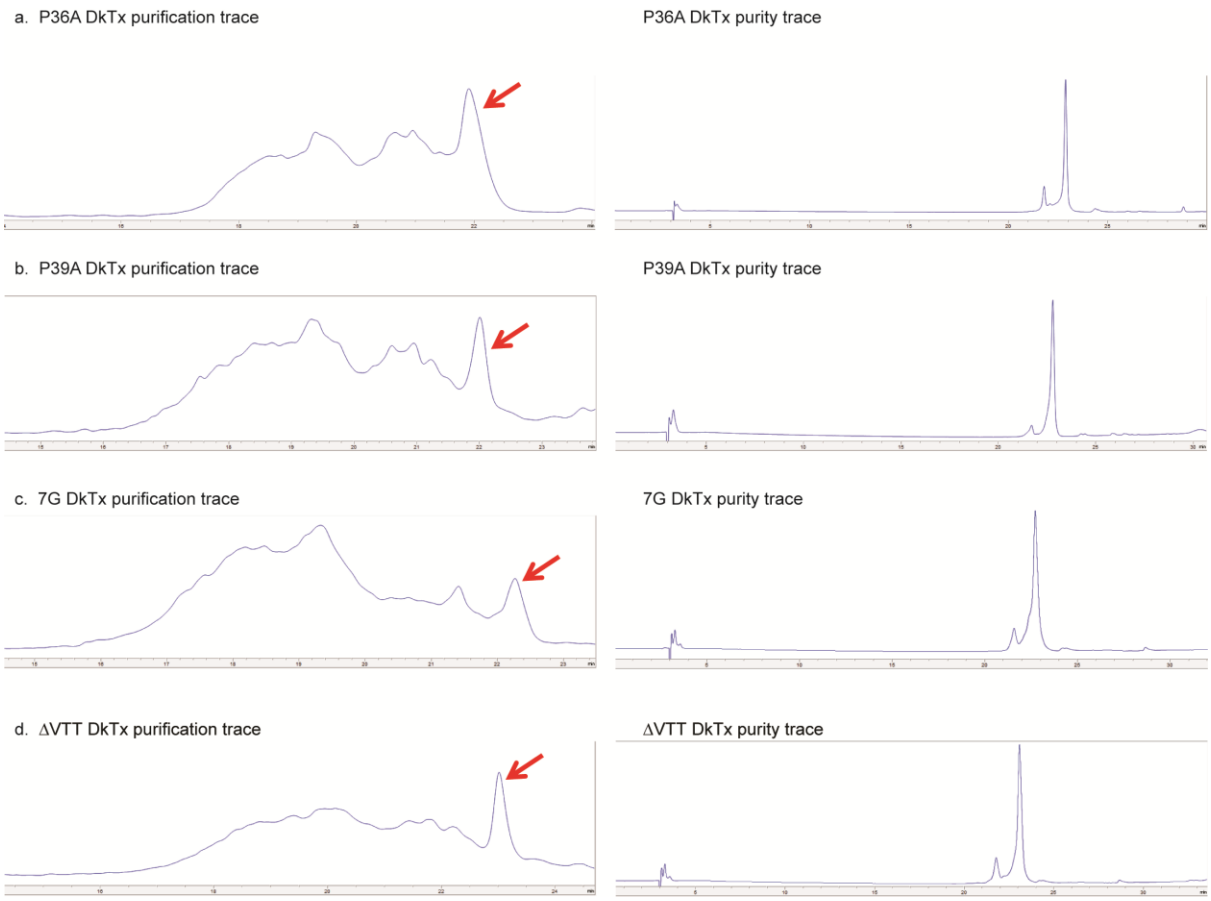

Figure 7: HPLC traces of purification and purity assessment of each of the 4 DkTx linker variants.

Proteins in the post-induction lanes (~24 kDa bands) corresponding to the fusion KSI-DkTx protein (Figure 6). The cells pellets were processed as mentioned in the 'protein production' section in the '*materials and methods*' section. The linear peptides in case of each of the mutants were folded *in vitro* in redox buffer (as mentioned in 'protein refolding and purification' section of *materials and methods*) and purified by RP-HPLC (Figure 7). The purified proteins were checked for sharp-peak in HPLC to designate purity (Figures 6) and also characterized for folded mass by MALDI-TOF mass spectrometry (presented in Table 1). These folded protein were then aliquoted and vacuum-dried as 1nmol aliquots for activity assays.

The wild-type DkTx showed a massive yield of 107 nmol from 10 mg of linear peptide. P36A showed very good refolding yield whereas ΔVTT and 7G DkTx showed refolding yield relatively poorer than P36A peptide. P36A DkTx protein refolding yielded 96 nmol from 10 mg linear peptide, whereas ΔVTT DkTx yielded 69 nmol from 30 mg of linear peptide and 7G DkTx yielded 48 nmol from 20 mg linear peptide. For P39A DkTx refolding yield was 7nmol from 10 mg linear peptide.

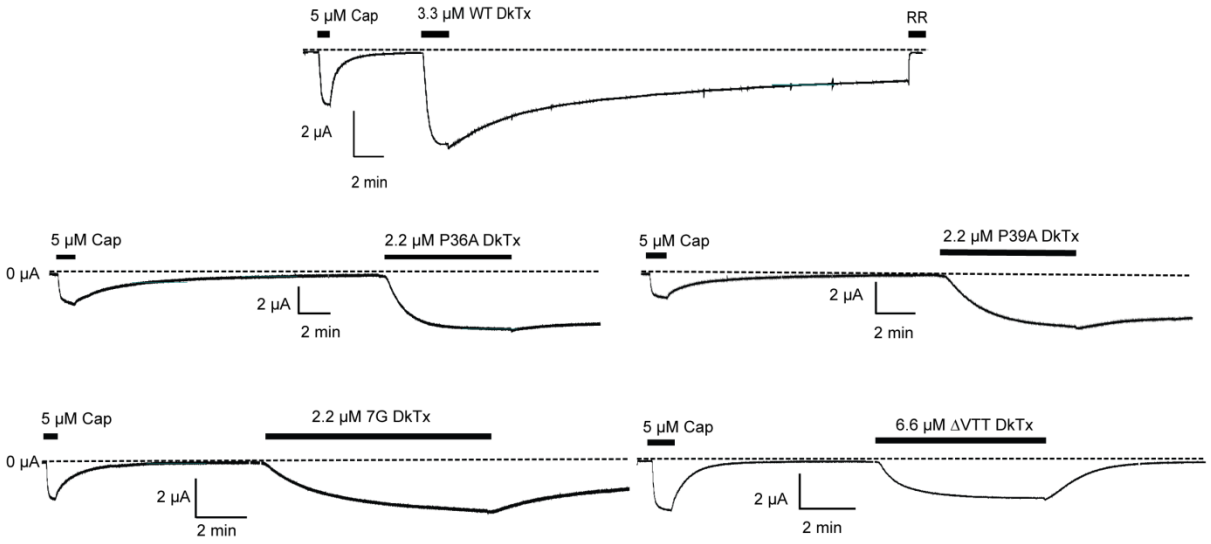

Figure 8: Two-electrode voltage clamp electrophysiology traces of wild-type DkTx and P36A, P39A, 7G and ΔVTT DkTx. Recordings were performed on *Xenopus laevis* oocytes held at -60 mV. Following 5 µM capsaicin application and complete wash-off of capsaicin current mentioned the concentration of wild-type DkTx or DkTx variants were pipetted in the recording chamber. For wild-type toxin trace, following 30 min wash-off, 7 µM ruthenium red was added to the recording chamber to block TRPV1 current.

Recordings from the wild-type (WT) DkTx and the two alanine variants P39A and P36A showed high potency and slow-wash off kinetics. The dose responses of both P36A and P39A DkTx were found to be nearly overlapping, and the EC_{50} of both were respectively 1.6 and 1.8-folds greater than that of the wild-type DkTx (Figure 9, Table 1). This minute difference hardly accounts for any significant variation of potency. When the wash-off kinetics was compared as percentage wash-off after 3 minutes, there was no significant difference found between the WT toxin and the alanine variants (Figure 10, Table 1). However, 7G DkTx showed a significant rightward shift in dose-response, resulting in nearly a 10-fold increase in EC_{50} (Figure 9, Table1). However, no drastic change of wash-off kinetics was observed for the 7G DkTx(Figure 10, Table 1). This result is consistent with the fact that 7G DkTx shows strong partitioning in lipid vesicles composed of POPC:POPG::1:1, similar to the wild-type DkTx.(Bae et al., 2016) Interestingly, the three amino acid deletion variant ΔVTT DkTx showed a strong rightward shift of the dose-response, resulting in nearly 157-fold higher EC_{50}(Figure 9, Table 1). Remarkably, another special feature that was observed for this variant was its unusual fast wash-off kinetics which is significantly higher than the alanine variants or the 7G DkTx (Figure 10, Table 1).

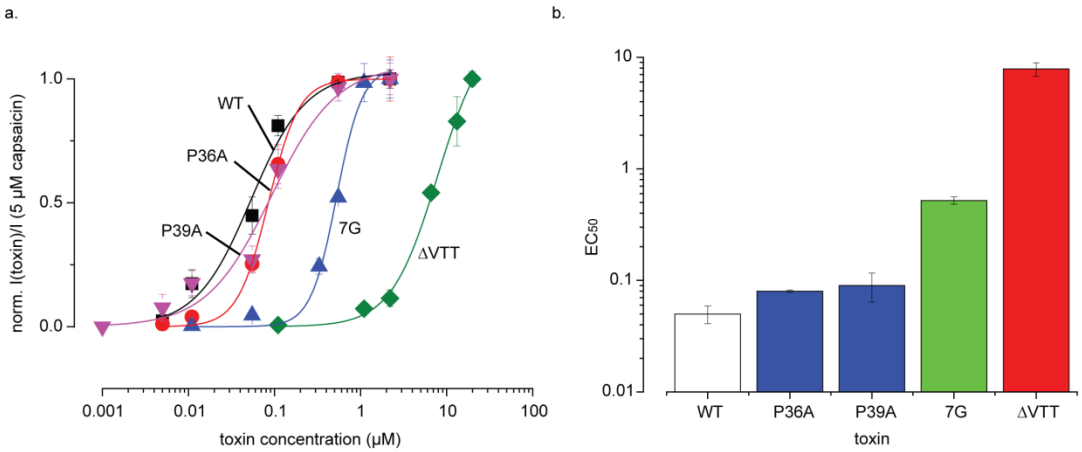

Figure 9: Dose-response and EC_{50} bar graph for DkTx linker variants. **a.** Dose-response of DkTx and its linker variants. P36A and P39A DkTx show near overlapping dose-response to wild-type DkTx. 7G DkTx shows 10-fold rightward shift and ΔVTT shows a 157-fold rightward shift of dose-response. **b.** Bar graph showing potency difference among DkTx linker variants compared to wild-typeDkTx.

Table 1:

DkTx variant	Retention time (min)	Expected Mass (a.m.u.)	Observed Mass (a.m.u.)	EC_{50} (µM)	n_H	% wash-off after 3 min
wild-type	22.9	8586.9	8582.8	0.05 ± 0.01	1.36 ± 0.33	23.92 ± 1.00 (0.55 µM)
P36A	22.8	8559.9	8553.5	0.08 ± 0.00	2.43 ± 0.20	30.56 ± 4.29 (0.55 µM)
P39A	22.8	8559.9	8559.7	0.09 ± 0.03	1.15 ± 0.35	37.61 ± 1.76 (0.55 µM)
ΔVTT	23.0	8284.6	8283.0	7.85 ± 1.08	1.60 ± 0.18	72.68 ± 3.61 (19.8 µM)
7G	22.7	8227.0	8225.5	0.52 ± 0.04	2.90 ± 0.59	42.91 ± 4.49 (1.1 µM)

Discussion

The double-knot toxin is high avidity TRPV1 channel binder that leads to prolonged activation of the ion channel. This phenomenon of the very tight interaction of DkTx

and TRPV1 has been strongly attributed to its bivalent nature of binding in previous literature (Bae et al., 2016; Bohlen et al., 2010). However, in our lab, we have demonstrated that strong lipid partitioning by DkTx and hence being present in the cellular membrane at a high local concentration near the target channel also contributes to the apparent high affinity of the toxin to the channel (Sarkar et al., unpublished data). Although detailed investigations have explored the role of the two ICK knots of the toxin in the TRPV1 activation mechanism is a reasonable amount of details, no study has yet aimed at exploring the role of the linker in DkTx mediated TRPV1 activation mechanism. This current study explores the role of linker region in DkTx mediated TRPV1 activation for the first time. Even though, in earlier studies length of linker region have been increased to separate two knots of DkTx by incorporating a Genenase I protease cleavage site “HYR” in the sequence of the linker, it was found that this increased length of linker region does not affect its channel activation properties (Bohlen et al., 2010; Sarkar et al., unpublished data). It is also reported that replacing the entire linker with seven glycines, thus making the linker very flexible, does not affect the membrane partitioning properties of the toxin. (Bae et al., 2016)However, the authors have not investigated the activation properties of the 7G DkTx. In my current work, I have performed functional studies on four linker variants of DkTx, namely P36A, P39A, 7G and ΔVTT employing two-electrode voltage clamp electrophysiology.

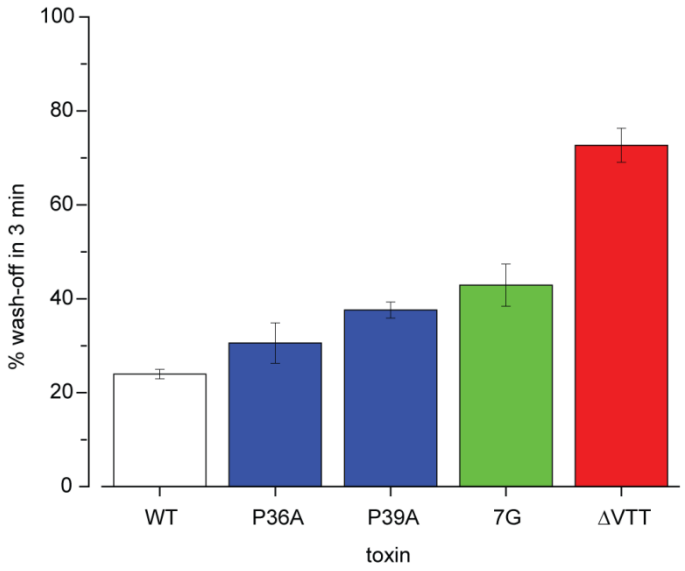

Figure 10: Wash-off kinetics of wild-type DkTx and its linker variants. Wash-off kinetics is expressed as percentage wash-off after 3 minutes of reaching maximal toxin–induced current.

<u>Linker rigidity has a lesser impact on function than the length of the linker</u>:

Study of activation characteristics of the proline to alanine substitutions indicates that it results in very little perturbation in the activation properties of the toxin. P36A EC_{50} was found to be 1.6-fold higher than wild-type DkTx (Figure 9, Table 1). Again for P39A variant also the difference is 1.8-fold, which indicates that rigidity of the linker region does not seem to play an important role towards the potency of the toxin towards activating TRPV1(Figure 9, Table 1). The 7G DkTx variant, on the other hand, demonstrates an EC_{50}value that is10-fold higher than that of wild-type DkTx (Figure 9, Table 1), suggesting that that the flexibility of the linker plays a major role in the toxin's binding to the channel. This result is also indicative of the fact that having the two knots placed at an equal distance as of the wild type DkTx might not be enough and the structural scaffold that holds them apart does bear a role in conferring potency. Remarkably, a huge rightward shift in dose-response for the ΔVTT variant, which is a three amino acid truncation variant of the linker region, shows the length of the linker plays a crucial role. An EC_{50} change of 157-fold compared to the wild-type toxin(Figure 9, Table 1) suggests that even if the toxin knots were to be correctly folded, they were not able to activate the channel to a complete extent.

Measuring wash-off kinetics properties of each of these four mutants indicated that the alanine variants of P36 and P39 do not alter the dissociation kinetics of the toxin from the channel. While the dose responses of P36A and P39A were nearly comparable to wild-type DkTx, all of the same saturates at 0.55 μM concentration. While we compared their percentage wash-off after 3 minutes (Figure 10, Table 1), we found the insignificant change in wash-off. Furthermore, when we incorporated the 7G DkTx (dose-response saturating at 1.1 μM) in the wash-off analysis (Figure 10, Table 1), we observed that even higher structural flexibility do not confer significant change of wash-off kinetics either. This is in a way consistent with the fact that 7G DkTx partitions comparable to the wild-type DkTx in the lipid vesicles composed of POPC:POPG::1:1. (Bae et al., 2016). Drastically, a significant change was observed with the ΔVTT variant. This variant exhibited a percentage change in wash-off of 72.6% at a saturation concentration of 19.8 μM(Figure 10, Table 1), whereas the toxin current gets washed off completely at concentrations as high as 6.6 μM (Figure 8 bottom right panel). This is suggestive of the fact that linker length plays a crucial role in the activation mechanism by placing the two knots in its correct

sites on the channel pore region. It is tempting to compare the results of this variant to the potency and wash-off properties of the W11 variants of DkTx, namely W11A and W11L, which show a similar drop in potency and fast wash-off kinetics. Even though the structural characterization of the ΔVTT variant with circular dichroism spectroscopy and its partitioning in artificial large unilamellar vesicles could be possible experiments to follow, yet it is appealing to speculate that maybe reduction in linker length makes both two knots of the toxin unable to bind to the channel binding sites at the same time and hence the toxin behaves like a single knot toxin in terms of potency and wash-off. Another intriguing hypothesis is that the truncated toxin variant does not partitions as well as the wild-type toxin and this disruption in membrane interactions of the toxin results in fast wash-off.

Summary and future directions

In summary, we have studied potency, and wash-off kinetics of P36A, P39A, ΔVTT and 7G DkTx that confers insight into the role of linker region in DkTx mediated TRPV1 activation. Results with the alanine variants convincingly discard the importance of any probable role of the prolines towards conferring rigidity to the toxin, which could be important to the channel activation mechanism. The ten-fold difference in potency observed in the case of the 7G variant suggests that the linker flexibility could have an impact on the toxin's potency. In future, experimenting with an α-helical rigid linker could be useful in studying this importance of flexibility. The drastic difference observed with ΔVTT DkTx emphasizes the significant contribution of the linker length. Yet to rule out the lack of partitioning in these fast wash-off ΔVTT DkTx variant, we have to perform tryptophan fluorescence based lipid partitioning experiments.

Designing further studies with one, two and four amino acid deletions from the linker and increasing the linker length to greater than ten amino acids long could contribute greatly to the better understanding of the role of the linker in the DkTx mediated TRPV1 activation mechanism. These results aid us to attribute importance to the yet unexplored role of the linker region in binding affinity and potency towards the channel.

References:

Adams, M.E., and Olivera, B.M. (1994). Neurotoxins: overview of an emerging research technology. Trends Neurosci. *17*, 151–155.

Alabi, A.R.A., Bahamonde, M.I., Jung, H.J., Kim, J. Il, and Swartz, K.J. (2007). Portability of paddle motif function and pharmacology in voltage sensors. Nature *450*, 370–375.

Andreev, Y.A., Kozlov, S.A., Koshelev, S.G., Ivanova, E.A., Monastyrnaya, M.M., Kozlovskaya, E.P., and Grishin, E. V (2008). Analgesic Compound from Sea Anemone Heteractis crispa Is the First Polypeptide Inhibitor of Vanilloid Receptor 1 (TRPV1) *. *283*, 23914–23921.

Bae, C., Kalia, J., Song, I., Yu, J., Kim, H.H., Swartz, K.J., and Kim, J. Il (2012). High Yield Production and Refolding of the Double-Knot Toxin, an Activator of TRPV1 Channels. PLoS One *7*.

Bae, C., Anselmi, C., Kalia, J., Jara-Oseguera, A., Schwieters, C.D., Krepkiy, D., Lee, C.W., Kim, E.H., Kim, J.I.I., Faraldo-Gómez, J.D., et al. (2016). Structural insights into the mechanism of activation of the TRPV1 channel by a membrane-bound tarantula toxin. Elife *5*, 1–30.

Bohlen, C.J., Priel, A., Zhou, S., King, D., Siemens, J., and Julius, D. (2010a). A bivalent tarantula toxin activates the capsaicin receptor, TRPV1, by targeting the outer pore domain. Cell *141*, 834–845.

Boukalova, S., Teisinger, J., and Vlachova, V. (2013). Protons stabilize the closed conformation of gain-of-function mutants of the TRPV1 channel. Biochim. Biophys. Acta - Mol. Cell Res. *1833*, 520–528.

Brieger L, (1883) Zur Erkenntnis der faulnisalkaloide, Beri Dtsch Chem Ges;16:1186-1191,1405-1407

Brieger L, Fraenkel C. (1890), Untersuchungen uber Bakteriengifte. Berlin Klin Wochenschr; 27:231-246,268-271

Cao, E., Liao, M., Cheng, Y., and Julius, D. (2013). TRPV1 structures in distinct conformations reveal activation mechanisms. Nature *504*, 113–118.

Caterina, M.J., Schumacher, M.A., Tominaga, M., Rosen, T.A., Levine, J.D., and Julius, D. (1997). The capsaicin receptor : a heat-activated ion channel in the pain pathway. *389*.

Chung, M.K., Güler, A.D., and Caterina, M.J. (2008). TRPV1 shows dynamic ionic selectivity during agonist stimulation. Nat. Neurosci. *11*, 555–564.

Gao, Y., Cao, E., Julius, D., and Cheng, Y. (2016). TRPV1 structures in nanodiscs reveal mechanisms of ligand and lipid action. Nature 1–17.

Garcia, M.L., Garcia-calvo, M., Hidalgo, L.P., Lee, A., and Mackinnon, R. (2000). Purification and Characterization of Three Inhibitors of Voltage-Dependent. 6834–6839.

Gaudet, R. (2008). A primer on ankyrin repeat function in TRP channels and beyond. Mol. Biosyst. *4*, 372.

Goldstein, S.A.N., Pheasant, D.J., and Miller, C. (1994). The charybdotoxin receptor of a Shaker K+channel: Peptide and channel residues mediating molecular recognition. Neuron *12*, 1377–1388.

Hille, Bertil.(2001) . Ion channels of excitable membranes (Sunderland:Sinauer assciates.Inc,)

Inada, H., Procko, E., Sotomayor, M., and Gaudet, R. (2012). Structural and biochemical consequences of disease-causing mutations in the ankyrin repeat domain of the human TRPV4 channel. Biochemistry *51*, 6195–6206.

Kalia, J., Milescu, M., Salvatierra, J., Wagner, J., Klint, J.K., King, G.F., Olivera, B.M., and Bosmans, F. (2015). From foe to friend: Using animal toxins to investigate ion channel function. J. Mol. Biol. *427*, 158–175.

Lee, C.W., Kim, S., Roh, S.H., Endoh, H., Kodera, Y., Maeda, T., Kohno, T., Wang, J.M., Swartz, K.J., and Kim, J. Il (2004). Solution structure and functional characterization of SGTx1, a modifier of Kv2.1 channel gating. Biochemistry *43*, 890–897.

Liao, M., Cao, E., Julius, D., and Cheng, Y. (2013a). Structure of the TRPV1 ion channel determined by electron cryo-microscopy. Nature *504*, 107–112.

Liao, M., Cao, E., Julius, D., and Cheng, Y. (2013b). Structure of the TRPV1 ion channel determined by electron cryo-microscopy. Nature *504*, 107–112.

Lim, K.M., and Park, Y.H. (2012). Development of PAC-14028, a novel transient receptor potential vanilloid type 1 (TRPV1) channel antagonist as a new drug for refractory skin diseases. Arch. Pharm. Res. *35*, 393–396.

Lin, Z., Chen, Q., Lee, M., Cao, X., Zhang, J., Ma, D., Chen, L., Hu, X., Wang, H., Wang, X., et al. (2012). Exome sequencing reveals mutations in TRPV3 as a cause of Olmsted syndrome. Am. J. Hum. Genet. *90*, 558–564.

Loukin, S., Su, Z., and Kung, C. (2011). Increased basal activity is a key determinant in the severity of human skeletal dysplasia caused by TRPV4 mutations. PLoS One *6*, 1–8.

McGivern, J.G. (2007). Ziconotide: a review of its pharmacology and use in the treatment of pain. Neuropsychiatr Dis Treat *3*, 69–85.

Mebb, D. (2002) . Venomous and poisonous animals: a handbook for biologists, and toxicologists and toxinologists, Physicians and pharmacists (Boca Raton: CRC press)

Milescu, M., Vobecky, J., Roh, S.H., Kim, S.H., Jung, H.J., Kim, J. Il, and Swartz, K.J. (2007). Tarantula Toxins Interact with Voltage Sensors within Lipid Membranes. *130*.

Moiseenkova-Bell, V.Y., Stanciu, L. a, Serysheva, I.I., Tobe, B.J., and Wensel, T.G.

(2008). Structure of TRPV1 channel revealed by electron cryomicroscopy. Proc. Natl. Acad. Sci. U. S. A. *105*, 7451–7455.

Nilius, B., and Owsianik, G. (2011). The transient receptor potential family of ion channels. Genome Biol *12*, 218.

Nilius, B., Owsianik, G., Voets, T., and Peters, J. a J. a. (2007). Transient receptor potential cation channels in disease.

Payandeh, J., Scheuer, T., Zheng, N., and Catterall, W.A. (2011). The crystal structure of a voltage-gated sodium channel. Nature *475*, 353–359.

Peigneur, S., Yamaguchi, Y., Kawano, C., Nose, T., Nirthanan, S., Gopalakrishnakone, P., Tytgat, J., and Sato, K. (2016). Active Sites of Spinoxin, a Potassium Channel Scorpion Toxin, Elucidated by Systematic Alanine Scanning. Biochemistry *55*, 2927–2935.

Ramsey, I. Scott., Delling, Markus., and Clapham, David E. (2006). An Introduction to TRP channels, Annu. Rev. Physiol. 68,619-47

Sarkar, Debayan., Singh, Yashashwi., and Kalia, Jeet. Protein–lipid interfaces drive TRPV1 ion channel activation by the double-knot spider toxin. (Unpublished data)

Siemens, J., Zhou, S., Piskorowski, R., Nikai, T., Lumpkin, E.A., Basbaum, A.I., King, D., and Julius, D. (2006). Spider toxins activate the capsaicin receptor to produce inflammatory pain. *444*, 1–5.

Suri, A., and Szallasi, A. (2008). The emerging role of TRPV1 in diabetes and obesity. Trends Pharmacol. Sci. *29*, 29–36.

Susankova, K., Ettrich, R., Vyklicky, L., Teisinger, J., and Vlachova, V. (2007). Contribution of the putative inner-pore region to the gating of the transient receptor potential vanilloid subtype 1 channel (TRPV1). J. Neurosci. *27*, 7578–7585.

Swartz, K.J. (2007). Tarantula toxins interacting with voltage sensors in potassium channels. Toxicon *49*, 213–230.

Appendix 1

Primers Design for Mutation in 7 residue linker region:

1. ΔVTT DkTx

ΔVTT F.P.: 5’ CCTTATGTTCCAAACTGTGCCAAAGAG 3’

ΔVTT F.P.: 5’ GGCACAGTTTGGAACATAAGG 3’

2. P36A DkTx

P36A F.P.: 5’ CTGTAAAAAATATAAAGCGTATGTTCCAGTAACCAC 3’

P36A R.P.: 5’ CTGGAACATACGCTTTATATTTTTTACAGTGC 3’

3. P39A DkTx

P39A F.P: 5’ CCTTATGTTGCGGTAACCACCAACTGTGCC 3’

P39A R.P: 5’ GGTGGTTACCGCAACATAAGGTTTATATTTTTTACAG 3’

Appendix 2

PCR protocols:

P39A:

95˚C for 1 minute	Initial denaturation
95˚C for 1 minute	25 cycles
60˚C for 1 minute	
72˚C for 4 minutes	
72˚C for 5 minutes	Final extension
4˚C till removal	Store

P36A:

95˚C for 1 minute	Initial denaturation
95˚C for 1 minute	25 cycles
52˚C for 1 minute	
72˚C for 4 minutes	
72˚C for 5 minutes	Final extension
4˚C till removal	Store

ΔVTT RF cloning PCRs:

PCR1 and PCR2

95˚C for 1 minute	Initial denaturation
95˚C for 1 minute	35 cycles
58˚C for 1 minute	
72˚C for 4 minutes	
72˚C for 5 minutes	Final extension
4˚C till removal	Store

PCR3

95˚C for 1 minute	Initial denaturation
95˚C for 1 minute	35 cycles
58˚C for 1 minute	
72˚C for 4 minutes	
72˚C for 5 minutes	Final extension
4˚C till removal	Store

PCR4

95˚C for 1 minute	Initial denaturation
95˚C for 1 minute	25 cycles
58˚C for 1 minute	
72˚C for 4 minutes	
72˚C for 5 minutes	Final extension
4˚C till removal	Store